NASA/TM–2018-219816

Small Unmanned Aerial System (UAS) Flight Testing of Enabling Vehicle Technologies for the UAS Traffic Management Project

Louis J. Glaab, Chester V. Dolph, Steven D. Young, Neil C. Coffey,
Robert G. McSwain, and Michael J. Logan
Langley Research Center, Hampton, Virginia

Donald E. Harper
Analytical Mechanics Associates, Inc., Hampton, Virginia

April 2018

NASA STI Program . . . in Profile

Since its founding, NASA has been dedicated to the advancement of aeronautics and space science. The NASA scientific and technical information (STI) program plays a key part in helping NASA maintain this important role.

The NASA STI program operates under the auspices of the Agency Chief Information Officer. It collects, organizes, provides for archiving, and disseminates NASA's STI. The NASA STI program provides access to the NTRS Registered and its public interface, the NASA Technical Reports Server, thus providing one of the largest collections of aeronautical and space science STI in the world. Results are published in both non-NASA channels and by NASA in the NASA STI Report Series, which includes the following report types:

- TECHNICAL PUBLICATION. Reports of completed research or a major significant phase of research that present the results of NASA Programs and include extensive data or theoretical analysis. Includes compilations of significant scientific and technical data and information deemed to be of continuing reference value. NASA counter-part of peer-reviewed formal professional papers but has less stringent limitations on manuscript length and extent of graphic presentations.

- TECHNICAL MEMORANDUM. Scientific and technical findings that are preliminary or of specialized interest, e.g., quick release reports, working papers, and bibliographies that contain minimal annotation. Does not contain extensive analysis.

- CONTRACTOR REPORT. Scientific and technical findings by NASA-sponsored contractors and grantees.

- CONFERENCE PUBLICATION. Collected papers from scientific and technical conferences, symposia, seminars, or other meetings sponsored or co-sponsored by NASA.

- SPECIAL PUBLICATION. Scientific, technical, or historical information from NASA programs, projects, and missions, often concerned with subjects having substantial public interest.

- TECHNICAL TRANSLATION. English-language translations of foreign scientific and technical material pertinent to NASA's mission.

Specialized services also include organizing and publishing research results, distributing specialized research announcements and feeds, providing information desk and personal search support, and enabling data exchange services.

For more information about the NASA STI program, see the following:

- Access the NASA STI program home page at http://www.sti.nasa.gov

- E-mail your question to help@sti.nasa.gov

- Phone the NASA STI Information Desk at 757-864-9658

- Write to:
  NASA STI Information Desk
  Mail Stop 148
  NASA Langley Research Center
  Hampton, VA 23681-2199

NASA/TM–2018-219816

Small Unmanned Aerial System (UAS) Flight Testing of Enabling Vehicle Technologies for the UAS Traffic Management Project

Louis J. Glaab, Chester V. Dolph, Steven D. Young, Neil C. Coffey,
Robert G. McSwain, and Michael J. Logan
Langley Research Center, Hampton, Virginia

Donald E. Harper
Analytical Mechanics Associates, Inc. Hampton, Virginia

National Aeronautics and
Space Administration

Langley Research Center
Hampton, Virginia 23681-2199

April 2018

Available from:

NASA STI Program / Mail Stop 148
NASA Langley Research Center
Hampton, VA 23681-2199
Fax: 757-864-6500

Abstract

Small unmanned aerial systems (sUAS) have been studied and results indicate that there is a large array of highly-beneficial applications. These applications are too numerous to list, but include search and rescue, fire spotting, precision agriculture, etc. to name a few. Typically sUAS vehicles weigh less than 55 lbs and will be performing flight operations in the presence of manned aircraft and other sUAS. Certain sUAS applications, such as package delivery, will include operations in the close proximity of the general public. The full benefit from sUAS is contingent upon the resolution of several technological areas to enable free and wide-spread use of these vehicles. Technological areas in question include, but are not limited to: autonomous sense and avoid and deconfliction of sUAS from other sUAS and manned aircraft, communications and interfaces between the vehicle and human operators, and high-reliability autonomous systems. The NASA UAS Traffic Management (UTM) project is endeavoring to develop a traffic management system and concept of operations for these types of vehicles. An extensive sUAS flight test effort was performed to partially address vehicle-related technological areas and to shape an understanding of future developmental and test efforts for vehicles intended to use the UTM traffic management system. The flight testing described herein had the following objectives: 1) Install and test Dedicated Short Range Communications (DSRC) systems developed for the automotive industry for potential sense and avoid sUAS applications; 2) Evaluate the use of cellular 4G systems to provide vehicle control; 3) Obtain high-resolution video imagery in support of image-based optical detection sense and avoid systems; 4) Acquire data in fixed-wing flight to support validation and maturation of an autonomous range containment system known as Safeguard in fixed-wing flight. A total of 53 flights were performed over 12 operational days at Beaver Dam Airpark in Elberon, VA. This work was sponsored by the UTM project that is part of the Aviation Operations and Safety Program (AOSP) at NASA.

Nomenclature

Amp Hour	Ah, unit of measure of the amount of battery capacity
AGL	Above Ground Level
ATC	Air Traffic Control
BVLOS	Beyond Visual Line of Sight
C2	Command and Control
CID	Cell tower ID
CONOPS	Concept of Operations
d	Computed distance between two GPS coordinates
DSRC	Dedicated Short-Range Communication systems
FAA	Federal Aviation Administration
FOV	Horizontal Field of View
GA	General Aviation
GCS	Ground Control Station
GCSO	Ground Control Station Operator
ID	Identification
IOD	Image-based Object Detection
λ	Difference in longitude for vehicles 1 and 2
LiPO	Lithium Polymer Battery
MR	Multi-Rotor
NAS	National Air Space
ppd	Pixels per degree
φ_1	Latitude for vehicle 1
φ_2	Latitude for vehicle 2
SAA	Sense and Avoid
sUAS	Small Unmanned Aerial System
R	Radius of the earth
R/C	Radio Control
RF	Radio Frequency
ROI	Region of Interest
RSO	Range Safety Officer
RSRP	Reference Signal Received Power
RSRQ	Reference Signal Received Quality
RTL	Return to Launch
UTM	UAS Traffic Management
WVLOS	Within Visual Line of Sight

Introduction

The introduction of small unmanned aerial systems (sUAS) into the National Airspace System (NAS) has been an objective of several efforts. It has been widely realized that sUAS (i.e.; those that weigh less than 55lbs) can provide tremendous benefit to mankind. Those benefits include a large and growing array of applications from traffic monitoring to fire spotting and even small package delivery. In order for sUAS to reach their full potential, several technological issues need be resolved in order to avoid exposing the general public to undue risks from sUAS operations. These risks include those involving mid-air collisions, both with manned aircraft as well as other sUAS, and also include risks associated with people and property on the ground. One area of technological development is a traffic management system that can deconflict sUAS from each other as well as provide general limitations to where the vehicles can operate to help partially mitigate, but not eliminate, the risk to manned aircraft. The NASA UAS Traffic Management (UTM) project has been developing a traffic management system for sUAS along with a concept of operations (CONOPS) as described in Reference 1.

Presently, the Federal Aviation Administration (FAA) permits limited within visual line of sight operations under Part-107 regulations. SUAS operators are permitted to operate their aircraft within visual line of sight (WVLOS) along with several other limitations such altitudes less than 400 ft above ground level (AGL), speeds less than 100 mph and operational locations sufficiently far away from airports. General WVLOS visual limitations range out to ~1 mile depending on the size of the vehicle. While WVLOS operations can provide substantial benefit and include applications such as construction monitoring, real estate, and limited precision agriculture and infrastructure monitoring and other tasks, substantially more valuable and beneficial applications require the sUAS to be operated beyond visual line of sight (BVLOS) and/or include multiple sUAS operated by a single person. Currently, the FAA does issue waivers to Part-107 requirements if the applicants can provide a valid safety case regarding their specific operation. Waivers are time consuming and comprehensive FAA regulations regarding routine BVLOS operations are needed. While a focus of the UTM project is on the development of a prototype UTM air traffic management system and associated CONOPS, efforts

within the UTM project to develop the required on-vehicle technologies are also being pursued.

While operating WVLOS, the human operator is responsible for assuring that the sUAS will not collide with manned aircraft or other sUAS, avoid overflight of unprotected people on the ground, and be able to intervene in the event of vehicle system issues. Operations BVLOS place an added emphasis on the vehicles' systems as real-time human intervention is much harder or even impossible in some situations.

Technological barriers to BVLOS and multi-sUAS per operator operations include, but are not limited to: 1) autonomous sense and avoid of other sUAS and manned aircraft, 2) communications and control, 3) highly-reliable autonomous systems, among other areas.

Elements that sUAS have in common with other aircraft are that they need to perform a mission within a certain level of risk and cost. Unlike other aircraft, sUAS are typically highly-limited by size, weight and cost and do not have human pilots onboard. In addition, some sUAS applications involve operations in very close proximity to the general public, such as envisioned for package delivery. Maintaining low-weight and size greatly contributes to mitigating the risk from the vehicle. However, in order to maintain low-weight, size, and cost, it is essential that sUAS leverage new and emerging micro technologies.

The testing conducted herein involves test and evaluations of several essential sUAS prototype subsystems. Objectives of the current test include: 1) Determine the usability of Dedicated Short Range Communications (DSRC) systems developed for the automotive industry for potential sense and avoid sUAS applications; 2) Evaluate the use of cellular 4G control systems to provide vehicle control; 3) Obtain high-resolution video imagery in support of image-based optical detection sense and avoid systems, and; 4) Acquire data in fixed-wing flight to support validation and maturation of an autonomous range containment system known as Safeguard in fixed-wing flight

While the UTM system will greatly mitigate the risk for mid-air collisions with manned aircraft by potentially establishing low-altitude sUAS operation areas, further mitigation is considered required since encounters with general aviation (GA) aircraft are still possible. Several options exist for sUAS sense and avoid (SAA) and include both ground-based sensing and onboard systems. Autonomous SAA for sUAS is considered critical to enable the vehicle to perform air traffic deconflictions.

Ground-based SAA systems have an advantage in that the ground based radar (or other sensors) do not have to be carried by the vehicle and with the advent of low-cost ground-based radars, as described in Reference 2, could feasibly be installed to provide usable areas of operations. A drawback of ground-based systems is that the communication link to the sUAS has to be extremely reliable since any type of communication failure would directly lead to a loss of SAA functionality for the sUAS and a mid-air collision hazard. The requirement for extremely reliable command and control (C2) links can lead to the C2 system being excessively heavy and/or expensive leading to an unviable sUAS.

Alternatively, onboard SAA systems allow some relief to the C2 requirement as the sUAS is able to both detect and then directly communicated with the autopilot to avoid airborne threats. Cooperative onboard SAA systems are exemplified by current Automatic Dependent Surveillance (ADS-B) systems used in manned aircraft. ADS-B systems continuously broadcast the vehicles' location to other aircraft and to ground-based transceivers that route the data to Air Traffic Control (ATC) (Reference 3). Aircraft equipped with both ADS-B in and out can also receive traffic information and use it to perform deconflictions. Currently, the ADS-B system is designed to handle envisioned commercial and GA traffic rates. The estimated number of future sUAS operations is considered high-enough to threaten to overload the radio frequency (RF) component and the ground based transceivers of the ADS-B system as presented in Reference 4. As such assuming ADS-B use (ADS-B out) for sUAS is not considered viable.

Alternatives to using typical ADS-B units for sUAS include greatly-reduced transmit power ADS-B units or other communications devices also described in Reference 4. It has been proposed to use DSRC systems as an alternative to ADS-B for sUAS. DSRC systems have been developed for the automotive industry to provide safety data links to drivers to warn of other vehicles and operate in the 5.9 GHz frequency band as described in Reference 5. It is envisioned that a DSRC-based sUAS SAA system could be used to deconflict sUAS from each other. It is also envisioned that this information could be received by ground-based stations and integrated with the FAA's ADS-B system. While some latency is possible with this concept, it could provide valuable awareness to manned aircraft pilots. Objectives of the current effort were to determine the performance of DSRC systems to provide air-to-ground, ground-to-air, and air-to-air communication links installed in representative sUAS. For this test, representative DSRC equipment was installed in sUAS and operated over ranges up to 0.5 miles (805 m) from the ground station. Multiple sUAS were operated with DSRC equipment installed for air-

to-air ranges from approximately 500 ft (152 m) up to 1 mile (1.6 km).

Command and control of sUAS is another critical challenge for BVLOS sUAS operations. One method of C2 involves direct communication link with the vehicle from the ground station. Typically this requires line of sight to the vehicle. Mountains, buildings, and trees could limit line of sight operations. Also, the power required to transmit increases dramatically as the range to the vehicle increases. Another option is satellite-based command and control as described in Reference 6. One challenge with this method is the size and power required to transmit data to/from satellites in orbit to sUAS. Recent developments include satellites with very large receive antennas that can help to reduce the transmit power required from the sUAS as discussed in Reference 6. Yet another C2 option involves terrestrial-based distributed communications technologies, such as 4G cell technology. A great advantage to this C2 method is the large amount of cellular infrastructure already in place as described in Reference 7. One concern with 4G cell C2 applications is that the system is designed to serve people on the ground with the cell tower beams aimed down slightly. Another concern is the method by which the system switches from one cell tower to another and the overall power and coverage available. In addition, local system overload is also possible is some urban environments. Lastly, latency issues with 4G C2 is yet another issue since this link involves multiple separate systems between the operator and sUAS. Reference 7 explores use of 4G C2 but focused only on the portion of the flight when the vehicle was at its' cruising condition. The current work endeavors to look at the entire sUAS operation including pre-flight, launch, climb, cruise, descent, landing, and post-flight recovery, in a rural environment.

Another option for onboard non-cooperative SAA for sUAS involves the use of visual-based sensors to provide detection of non-cooperative targets. Within this method high-resolution cameras provide video imagery to image-based object detection (IOD) algorithms. These algorithms also receive aircraft state data from the autopilot and can search for and detect airborne objects as discussed in Reference 8. Primary challenges for IOD algorithms are having enough pixels on the target for detection along with having adequate processing power available on the sUAS for effective tracking. Recent manned aircraft studies as documented in Reference 9 were performed in support of several applications. One potential application is for supersonic business jet aircraft, whose pilots may not have direct forward vision. Another application is for large UAS. A major challenge for IOD from sUAS applications are the extreme size, weight, power, constraints. Given the very low-altitude operational environment for sUAS compared to manned aircraft, testing was performed herein to determine the effect of extreme background clutter for IOD algorithms as compared to results from Reference 9. For this effort high-resolution cameras were affixed to sUAS and flown in the presence of another sUAS at ranges from approximately 500 ft (152 m) up to 1 mile (1.6 km).

Highly-reliable autonomous systems are required for BVLOS operations. SUAS feature many subsystems, such as navigation, control, batteries, sensors, C2, etc., which all will need to be highly-reliable for the entire sUAS to be highly-reliable. However, if the vehicle could be ensured to stay within a specific boundary, or outside of specific boundaries, then potentially the other subsystems could be allowed to perform at a lower-level of reliability and still result in an acceptable overall level of risk for limited BLVOS operations. Current geo-fencing, or geo-limitation, systems are designed to detect and warn with sUAS are outside of specified areas. For example, it is particularly useful to guard against inadvertent fly-aways caused by incorrect flight paths entered by the user or a lost link situation. Typically, these geo-fencing functions are implemented as embedded functions within the autopilot system; this effectively makes their reliability only as good as the reliability of the entire auto-pilot.

A system referred to as Safeguard was devised and developed with the intention of being independent of the auto-pilot and subject to rigorous software development and testing processes as described in References 10 and 11. The idea is to create a conformance monitor whose reliability can be much greater than the system it is monitoring. Extensive previous testing of Safeguard prototypes was accomplished using multi-rotor (MR) vehicles with top speeds of approximately 20 mph (10 m/s). It was desired to test Safeguard at higher flight speeds and on fixed-wing aircraft where aerodynamics are significantly different (e.g. when predicting ballistic trajectories). Safeguard-specific objectives for this flight test were (a) to confirm that installation, operation, and procedures were feasible and practical for fixed-wing sUAS, and (b) to collect Safeguard performance data at representative speeds and maneuvers for fixed-wing sUAS. Test data were acquired while operating at various speeds from 17 to 25 m/s (38 to 56 mph) at constant altitudes. Testing on other platforms is ongoing concurrently, with results to be published separately.

Method

To achieve all the objectives stated above a series of sUAS vehicles were modified to carry various components and then flown, either individually, or in pairs. A total of six sUAS were used for this effort. Vehicles used included a 120" span commercial Tempest sUAS, a 6-rotor MR referred as the Tarot Hexacopter, and a 68" span Mig-27 scale foam aircraft referred as the Mig.

Vehicles used

UASUSA Tempest

The Tempest UAS is an electrically-powered fixed-wing aircraft. The Tempest is manufactured by the UASUSA Company. It is launched via a rail and bungee cord system with an empty gross takeoff weight of 15 lbs. and belly-landed. The Tempest can carry up to 10 lbs. of payload and fly for over an hour on a single 11 Ah 5-cell Lithium Polymer (LiPO) battery. The baseline aircraft comes equipped with Pixhawk autopilot and long-range 900 MHz telemetry and 2.4 GHz radio control (R/C) links. While the vehicle is capable of fully autonomous launches and landings, it was manually flown for launches and landings for the flight testing performed herein. The Tempest was switched into autonomous mode (auto mode) when it was near the desired operating altitude and monitored by the safety pilot.

A total of two Tempest aircraft were used for the current testing. One Tempest (N533NU) was configured to carry the Safeguard geofencing system. Safeguard was self-contained, had its own battery power and only required a place to mount inside the vehicle. While being designed to interface with the vehicle's autopilot, the tests described here performed as a ride-along to acquire data at speeds and along flight paths more typical for fixed-wing sUAS. Additional details on the installation of Safeguard into N533NU are provided in a later section.

The other Tempest (N534NU), shown in Figure 1, was configured to carry a Bendix-King KGX-150 ADS-B unit, Botlink 4G cell and DSRC communication links in addition to the baseline equipage. With the potential addition of cameras, it is considered that the Tempest represents a viable commercial UTM sUAS platform and could perform fire spotting or other surveillance BVLOS missions. For the current research flights, the ADS-B unit was not powered to mitigate any potential effect on the DSRC testing. Further testing is anticipated to examine ADS-B effects on DSRC performance.

Figure 2 illustrates the installation of Botlink XRD in the aft payload bay of the Tempest aircraft. Provisions to enable the Pixhawk to control power to the Botlink XRD in flight were implemented to protect against potential failure modes. The antenna used for the Botlink was the Taoglass FXUB66. The Taoglass antenna was selected due to its very small size and easy compact mounting as compared to the standard dipole antennas. The antenna was mounted to the surface of the fuselage just aft of the wing as shown in Figure 3. The radiation pattern for the antenna is at 925 MHz is presented in Figure 4. Note that the Botlink operational frequency was 1.08 GHz. The "z" axis is aligned normal to the flat surface of the antenna and the "x" axis aligned with the longer dimension.

To provide essential safety of flight position awareness for potential BVLOS flight operations, a Bendix-King KGX-150 was installed in the Tempest. The KGX-150 is shown in Figure 5. It was installed in the forward payload bay and was powered by a dedicated 4cell 1,400 mah LiPO battery pack. The KGX-150 transmitted aircraft position on 978 MHz frequency at 40 Watts of power. A unity gain antenna was mounted in the canopy. Provisions were provided for the Pixhawk to control the power to the KGX-150 and be able to turn it on and off in flight to mitigate initial concerns regarding interference with other avionics. Testing indicated acceptable operations and at no time was there a need to shut-down the system in flight.

The OBU-201 DSRC unit was installed in the forward payload bay of the Tempest directly above the KGX-150 ADS-B as shown in Figure 6. Similar to the Botlink installation, a Taoglass MAXIMUS FXUB66 antenna was used shown in Figure 7. The radiation pattern of the antenna at 5.9 GHz is presented in Figure 8. Note in Figure 8 that the radiation pattern indicates some non-uniformity but does provide approximately 4 dB normal to the surface.

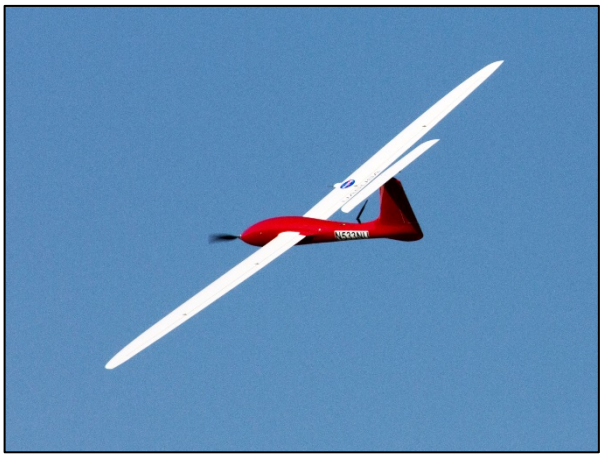

Figure 1 - Tempest-2 (N534NU) in flight.

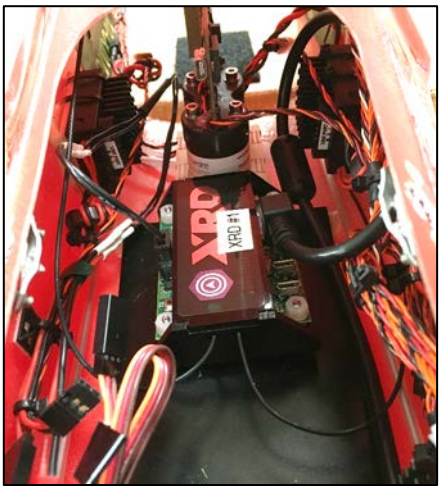

Figure 2 - Photograph of Botlink XRD device in the Tempest aft payload bay.

Figure 3 – Tempest fuselage illustrating installation of antennas for the Botlink (aft) and Unex OBU-201 (forward).

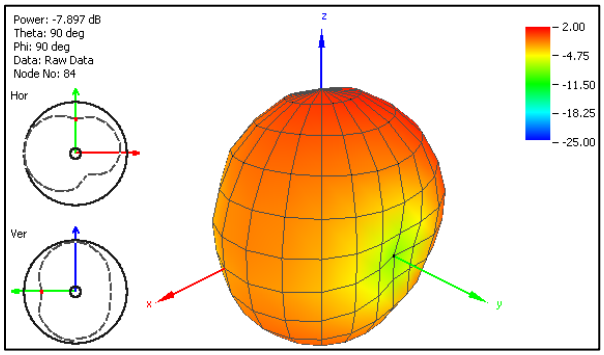

Figure 4 - Radiation pattern for FXUB66 Taoglass antenna at 925 MHz used for the Botlink.

Figure 5 - Bendix King KGX-150 ADS-B unit.

Figure 6 - Installation of the Unex OBU-201 in the Tempest.

Figure 7 - OBU-201 patch antenna.

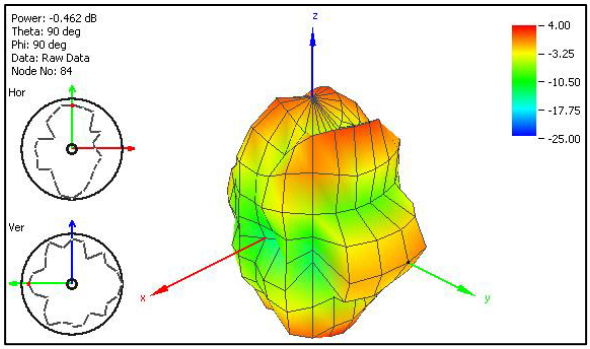

Figure 8 - Taoglass FXUB-66 antenna 5.9 GHz radiation pattern.

Tarot Hexacopter

The Tarot hexacopter MR has a rotor span of 40" and weighed approximately 15 lbs. in its research configuration. The Tarot used a 6 cell 16 Ah LiPO battery with a maximum flight time of approximately 16 minutes with 30% battery reserve. A 900 MHz telemetry link was used to control the vehicle from the GCS. In addition, the Tarot's also included R/C control via 2.4 GHz Spektrum system. Two Tarots were used for this effort. Both were equipped with Unex OBU-201 DSRC devices carried below the main body of the vehicle. A photograph of Tarot-1 is provided in Figure 9.

Figure 9 – Tarot Multi Rotor hexacopter.

Mig

The Mig vehicles are scale models of Russian Mig-27 ground attack aircraft. They were originally designed to serve as target practice vehicles for the US Army and are primarily constructed from foam. They were given to NASA and used for general testing purposes. The Mig's are general purpose vehicles and can carry approximately 5 lbs. of payload and fly for 15 minutes. They are electrically-powered conventional aircraft that takeoff and land under manual R/C pilot control. They were equipped with Pixhawk autopilots and could perform autonomous flight maneuvers.

Two Migs were used for the testing conducted herein. One was primarily a pilot proficiency trainer aircraft and referred to as Mig-CC. The other Mig, referred to as Mig-LH, was configured to carry cameras on the wing tips for IOD testing as well as carry an OBU-201 DSRC unit underneath the fuselage. A photograph of Mig-LH is presented in Figure 10. The installation of the OBU-201 DSRC unit onto Mig-LH is provided in Figure 11.

Figure 10 - Mig-LH.

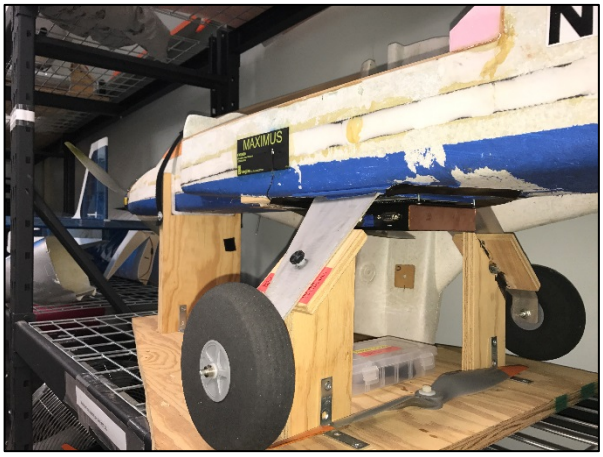

Figure 11 - Mig-LH fuselage with OBU-201 unit installed.

DSRC equipment

The Unex OBU-201 DSRC system was selected as a representative DSRC systems and used for testing. The OBU-201 basic system is shown in Figure 12. It was selected for testing as it was packaged in a robust enclosure that fit well into an array of sUAS platforms, user interface software was easy to use with good

customer support, and it met the DSRC requirements for frequency and power.

The transmission power for the OBU-201 system was measured to be 26 dB at a frequency of 5.86 GHz. The DSRC units were programed to transmit at 2 Hz when a 3D fix was determined at a data rate of 12 Mb/sec. Implementation testing revealed that the actual packet transmission rate was approximately 1.5 packets/sec. Only aerial packets are included in the airborne DSRC packet transmission analysis, i.e. both vehicles are airborne for flight test results. Ground testing evaluated packet transmission with the test vehicles stationary. Packet content includes: Call Sign, Latitude, Longitude, Altitude, Heading, Horizontal Velocity, Vertical Velocity, GPS HDOP, GPS Satellites in view, and GPS Satellites used in 3D fix calculation.

Four transmission paths were evaluated for testing documented herein: Ground to Ground, Vehicle to Ground, Ground to Vehicle, and Vehicle to Vehicle. Each transmitted packet was checked for successful reception by the other DSRC boxes. The transmitted packet timestamp was used to lookup GPS coordinates of the other DSRC boxes during a post-processing calculation of separation distance between the DSRC boxes using the Spherical Law of Cosines coordinates as shown in the formula below where d is the computed distance between the two GPS coordinates, φ_1 is the Latitude for vehicle 1, φ_2 is the Latitude for vehicle 2, λ is the difference between Longitude 1 and 2, and R is the Earth's Radius of 6,371 kilometers. Note that the d is ground distance and does not consider changes in elevation for distance calculations:

$$d = \cos^{-1}(\sin\varphi_1 * \sin\varphi_2 + \cos\varphi_1 * \cos\varphi_2 * \cos\lambda) * R$$

Figure 12 - Unex OBU-201 DSRC device with standard dipole antennas.

4G Cell Link

One objective of this flight test effort was to characterize the performance of 4G cell link systems to provide command and control of sUAS. To meet this objective a Botlink XRD unit was installed in the Tempest aircraft and configured to record cell link characteristic data at 1 HZ.

The 4G Botlink system is designed to be a communication link for sUAS. It includes an internet-connected tablet device with user interface and 4G transceiver onboard the aircraft that is connected to the Pixhawk autopilot. Data regarding the 4G cell link is recorded onboard an SD card internal to the Botlink device on the vehicle. Parameters recorded included: Reference Signal Received Power (RSRP), Reference Signal Received Quality (RSRQ), Tower ID for both the connected and neighboring towers, vehicle GPS latitude, longitude, and altitude, along with other parameters that describe the quality of the cell link. Cell link data were analyzed from approximately 60 seconds prior to launch to 60 seconds after landing.

A cell phone tower database was acquired with support from a wireless carrier. The general characteristics of the database are presented in Table 1 which presents the total number of cell phone towers in the database, the distance to the closest cell phone tower to the Beaver Dam test site, the distance to the tower furthest away, the average distance, and the standard deviation of the distance to the cell phone towers. Note that each cell phone tower generally includes three sectors with sector 1 aligned to the North, sector 2 to the South East and Sector 3 to the South West. Results are presented only for what specific tower was being communicated with and not which sector. In general, the cell coverage at Beaver Dam for surface use is considered to be commensurate with rural areas with very poor service based on users' experience at that facility.

Table 1 - Characteristics of cell phone tower database.

Total number of towers	16
Minimum range	5.2 miles
Maximum range	17.4 miles
Average range	11.5 miles
Standard deviation	4.2 miles

Image Object Detection

Provisions were made to also carry a high-resolution Sony Action Cam camera with narrow field of view lens on the Mig and Tarot vehicles. An image of the Sony Action Cam is provided in Figure 13. The Sony Action Cam camera featured a sensor resolution of 3840 horizontal by 2160 vertical pixels. To achieve very-high resolution imagery, a 41-deg horizontal field of view (FOV) lens. This combination produced a 93.7 pixel per degree (ppd) resolution. It should be noted that nominal 20/20 human visual acuity is defined as 60 ppd. Selecting a narrow FOV lens enhanced the number of pixels that could be put onto a target. More pixels on target enhances the ability for IOD algorithms to detect and track targets.

The work described here is an extension of the work previously published in Reference 8 with a revised 4k camera configuration from the stock fish-eye 170 degree FOV lens. This new lens configuration dramatically increased the number of pixels on the intruder aircraft that only yielded limited detection results above the horizon using an optical flow based algorithm. The motivation for this revision is to provide more image features on target for optical based detection and classification at greater separation distances and against more cluttered backgrounds (e.g. trees) that exist below the horizon. The same method from Reference 8 is currently being applied to achieve a baseline result and is presented in the Figure 1.

Figure 13 - Sony action cam.

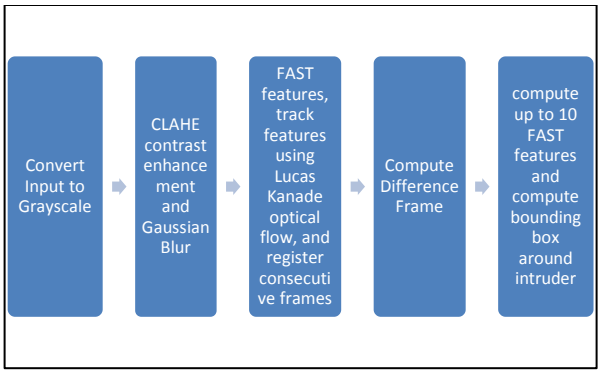

Figure 14: Optical flow based sUAS detector

Safeguard

The Safeguard system was designed to operate on any sUAS to provide highly-assured vehicle containment within, or exclusive of, specified areas as described in References 11 and 12. It was also designed to operate as an independent "black box", such that it could be readily installed and integrated into off-the-shelf aircraft. While the system has been evaluated extensively on MR sUAS at speeds and maneuvers commensurate to those vehicles and the missions they fly; it had yet to be installed, integrated, or tested on a fixed-wing sUAS like the Tempest. In addition to stressing the fit check to a tight SWAP conformance limit, the Tempest fixed-wing sUAS provided the ability to operate at twice the speeds of the MR sUAS, and for extended periods of time.

As shown in Figure 15, the Tempest-1 aircraft was configured to carry the prototype Safeguard unit. This required removing the outer case, repackaging into a smaller case, and moving the external connectors to be accessible for pre-loading and off-loading data.

Figure 15 – Safeguard installation in Tempest-1 aircraft.

In addition to the flight component of Safeguard, there is a user interface hosted on a laptop at the GCS. Although there is no connection to the unit during flight, this interface enables configuration (prior to flight) and data off-loading (post-flight) via a standard wired Ethernet connection.

Figure 16 is a screenshot of the graphical user interface from the version used during the testing. Several capabilities are implemented here, primarily to support developmental tests and software verification and validation. Operationally, the procedure for configuring the unit is straight-forward, taking only 2-3 minutes.

(1) Establish Ethernet connection
(2) Check error log from previous flight
(3) Perform system reset
(4) Load stay-in boundary
(5) Load stay-out boundary(s) (if any)
(6) Set/check mode (nav sys 1, nav sys 1+2)
(7) Set/check buffer scale factors
(8) Set/check aero coefficients
(9) Perform altitude initialization (Alt Init)
(10) If “all green”, then “operational”
(11) Unplug connector, ready to fly

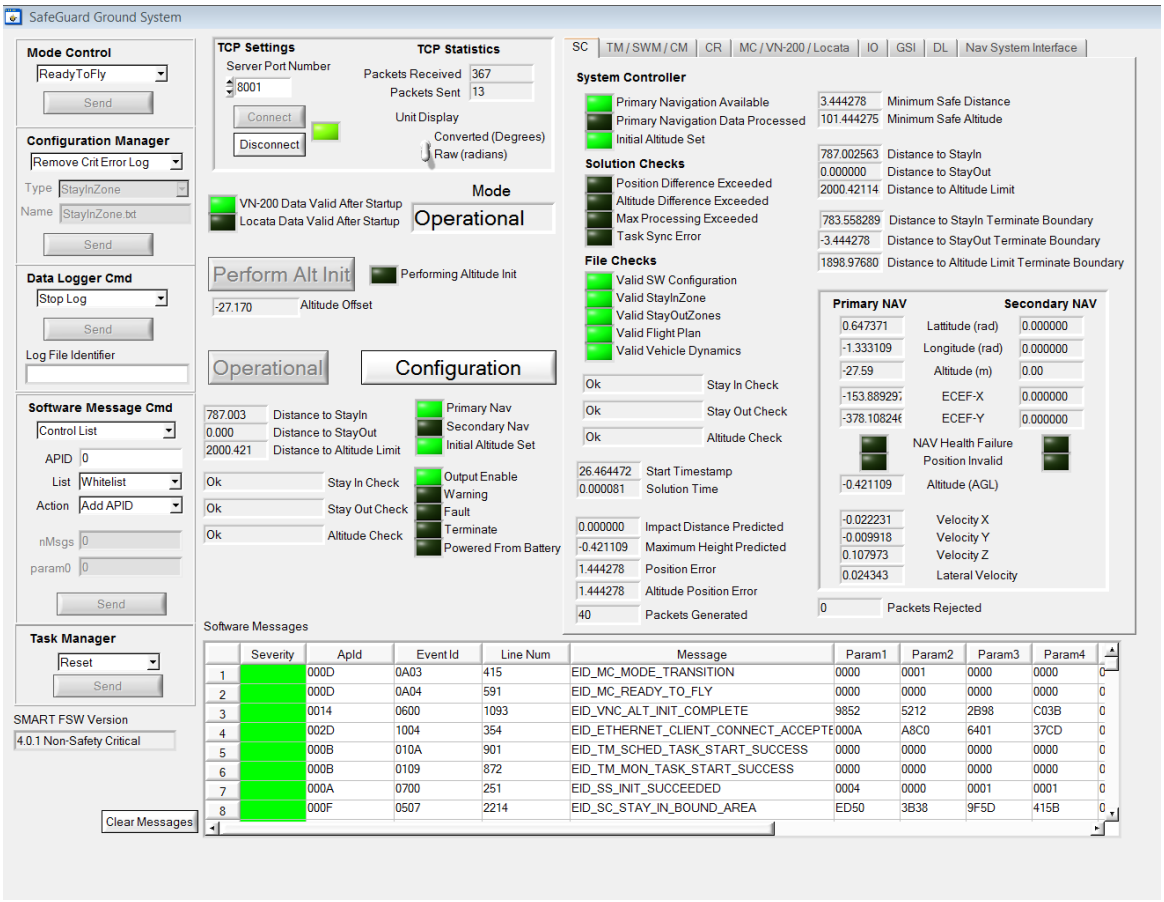

Figure 56: Safeguard user interface (developed by NASA Langley's Flight Software Systems Branch)

Ground testing and preparations

All vehicles were developed following a phased integrate test fly approach. This method allowed insight into vehicle integration for the various components to be understood one at a time. This method alleviates a situation where all systems are integrated at one time and evaluated all at once which can lead to significant delays due to a lack of understanding of the integration effects of one subsystem on another. It also allows more time operating the subsystems integrated into the vehicle earlier to build confidence in their operation and results and experience operating the systems.

Part of the ground testing performed involved ground range tests of the DSRC equipment. For this test the flight vehicles were assembled and all subsystems powered-up. However, no power was provided for the electric motors. This replicated to a large extent the electromagnetic environment on the vehicle in flight. A road segment was identified on NASA LaRC that was approximately 0.7 miles long and nearly completely straight and level. The vehicles were located at one end of the road and placed upon vehicle setup stands or plastic tables. Another DSRC box was located in a simple cardboard box with antennas and battery power and held by an operator. This DSRC box was referred to as the Mobile Unex box. The operator would then walk to the far end of the road and back again.

For the ground testing the Tempest vehicle was oriented pointing roughly North with the test range oriented in a Westerly direction. The Tarot was oriented in a Westerly direction with a clear view of both omni antennas to the Mobile Unex box. The Mig aircraft was tested in two orientations (North and West (Offset orientation)).

Flight test operations

For multi-vehicle operations, both aircraft were preflighted simultaneously by separate flight teams. Each vehicle flight team included a pilot, visual observer, and GCS operator (GCSO). In addition to each flight team, a range safety officer (RSO) was present to observe the flight operations. Once both aircraft were ready for flight they were moved to their specific launch locations.

The Tempest aircraft was referred to as the "target" aircraft and Mig and Tarot were considered to be "ownship" aircraft. All the ownship aircraft flew the Beaver Dam East route illustrated in Figure 17 at an altitude of 200 m (613 ft) AGL. The Tempest always flew the Beaver Dam West route illustrated in Figure 17 at altitudes of 170, 200, or 230 m (558, 613, 745 ft) AGL depending on the desired data to be acquired.

Conducting operations in this manner produced the following desired test attributes: 1) Produced a range of separation distances between the target and ownship aircraft from approximately 500 ft (152 m) up to 1 mile (1.6 km), 2) Produced a range of visual cross sections for the target vehicle across a range of separation distances, 3) Provided at, above, and below the horizon encounters and a range of altitudes for the IOD, and 4) Created a range of altitudes for the 4G cell link evaluation.

A run log of all the flights completed in support of this project are provided in Appendix A.

Tempest operations

For all multi-vehicle operations the Tempest was rail-launched first to leverage its longer endurance capabilities compared to the other aircraft. Once the vehicle was airborne it was manually flown to an altitude close to the desired target altitude and speed and aligned with the desired flight path then transitioned into auto mode. The Tempest would perform counter-clockwise flight paths maintaining constant airspeed and altitude. The airspeed used for most of the Tempest operations was 19 m/s (42.5 mph) which is approximately its maximum endurance speed. Safeguard operations included a range of speeds from 18 m/s to 25 m/s (40 to 58 mph). Once the Tempest was established in auto mode, the other vehicle was launched. After the other vehicle was landed and moved off the runway, the Tempest pilot would select manual flight mode and manually land the aircraft. In general, the Tempest flight times were approximately 25 minutes in duration.

Mig operations

The Mig was ground-launched and manually flown by the pilot. Altitude was limited to be approximately 300 ft (91 m) or less until the Mig was within its designated airspace east of the No Fly Zone shown in Figure 17. Once within its airspace, the aircraft was flown to its approximate target altitude and airspeed and aligned with the intended flight path. At that time, it was transitioned into auto mode and it would then execute clockwise flight paths. Altitude and airspeed were maintained during auto mode. The Mig was commanded to fly at 18 m/s (40.3 mph) which approximates its maximum endurance speed. When the flight time limit was reached, the Mig pilot would select manual flight mode and manually land the aircraft. At least a 30% battery reserve was maintained at all times.

Tarot operations

For flight operations with other aircraft the Tarot's flight plan included a region of interest (ROI) that would keep the vehicle aimed at a point in the distance that would keep it pointing in the general direction of the target aircraft. The Tarot was launched in manual mode then transitioned into auto mode. Once in auto mode the Tarot would maintain constant ground speed and altitude while maintaining orientation with the ROI. Ground speed used for the Tarot operations was 10 m/s (22.4 mph). Once the flight time limit was reached the pilot would either select return to launch (RTL) mode and the vehicle would autonomously fly to the point where the vehicle was powered-up and land itself.

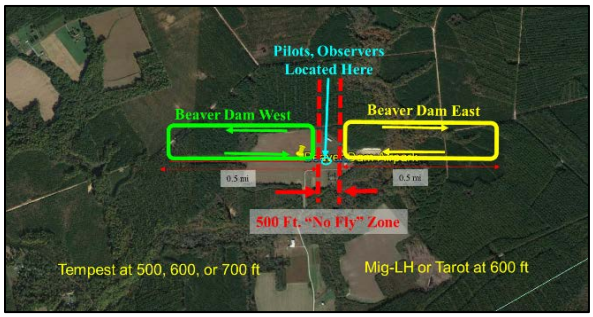

Figure 17 - Overview of routes flown.

Results and Discussion

Results are presented in the next 4 subsections for DSRC performance testing, 4G Botlink characterization, IOD discussion and some initial results and Safeguard evaluation results and discussion.

DSRC system testing

Results for DSRC V2V testing are provided in this section. Ground test results are presented first followed by flight test results.

DSRC ground testing

Initial ground range test results performed in November, 2017 are provided in Figure 18. The objective of the ground testing was to verify nominal performance before initiating flight operations. In Figure 18 the percent of packets transmitted from one DSRC device and received by another are presented along with the distance between the two devices.

From Figure 18 it can be seen that for separation distances less than 200 meters nearly 100% of the packets transmitted from the Mobile Unex box to the Tempest (N534) were received. Similarly, the packets transmitted from the Tempest to the Mobile Unex box were also received. As the separation range increased beyond 300 m the percent packets received began to decrease and reached 50% at approximately 600 meters. As range increased the percent of packets transmitted to or received by the Tempest (N534) reached zero by approximately 700 m.

Similar to the Tempest results, the Mig in the offset orientation (i.e. aligned with the test track) also received nearly 100% of the packets received at ranges less than 300 m. Packets transmitted from the Mig in the offset orientation were also received by the Mobile Unex box up to 300 m. As range increased beyond 300 m the percent of packets received decreased, similar to the Tempest, reaching 50% around 500 m and zero percent by 700 m.

Results for the Mig in the North orientation were substantially different than the Tempest and Mig in the offset orientation. For this test condition, the percent packets transmitted and/or received started out at only approximately 65% at close range and remained constant out to approximately 500 m. Beyond that range the percent packets transmitted and/or received dropped off also reaching near zero percent at 700 m.

The results for the Tarot transmitting to/from the Mobile Unex box were different from the other results. For ranges less than 300 m, the percent of packets received from the Tarot to the Mobile Unex box was approximately 95% up to 300 m range. Instead of dropping off as the results for the Tempest and Mig in the offset orientation, the percent of packets received from the Tarot to the Mobile Unex box remained much higher and was never less than 50% over the ranges tested out to 1.1 km. The percent of packets received by the Tarot from the Mobile Unex box were never above 50% but decreased at a rate similar to the results for the percent packets received by the Mobile Unex box from the Tarot.

It appears that the results for the Tempest, both for transmission and reception of packets, indicate somewhat consistent distributions with both transmission paths being similar to each other. Results for the Mig in the offset orientation (aligned with the test track) were similar to the Tempest. However, results for the Mig in the North heading orientation were very different. It is hypothesized that the presence of a carbon reinforcement strip located just beneath the Taoglass antenna confounded the DSRC installation and blocked emissions normal to the surface of the antenna. This blockage would have degraded transmission and reception in the direction of the test track and Mobile Unex box when the Mig was oriented in the North direction. This blockage was largely avoided for the offset (West) orientation. Results for the Tarot were unexpected and somewhat

unexplained. It is hypothesized that as a result of the Tarot being positioned approximately 2 ft off the ground, compared to 3 or 4 ft off the ground for the Mig and Tempest, that some type of ground interference or multi-path phenomena could have confounded the results.

The primary observations from the ground testing is that the percentage of packets transmitted between Unex DSRC boxes is nearly 100% for ranges below 300 m and decreases rapidly and range increases reaching 50% transmission at 500 m. Very low percentages of packets were received for ranges greater than 700 m in general.

DSRC Flight Testing

Figure 19 presents the distribution of data packets transmitted for all flights combined for ground-to-air, air-to-ground, and air-to-air. Range of test conditions achieved varied from as close as 100 m (328 ft) for air to ground and ground to air transmission paths and up to approximately 0.9 km (2,953 ft). Air to air transmission paths were evaluated from as low as 200 m (656 ft) up to 1.6 km (5,250 ft). Figure 19 is presented to provide some insight for the subsequent data analyses that involve the percentage of packets received. For the ground-to-Tempest and Tempest-to-ground the total number of data packets transmitted was approximately 800 to 900 for ranges from 0.3 out to 0.9 km. A somewhat lower number of packets were transmitted for the Mig to/from the ground since that vehicle had shorter flights and fewer flights than the Tempest. An even lower number of packets were acquired for the Tarot. Note that the max range of the Tempest to the ground station was slightly larger than for the Mig or Tarot due to the flight plans selected. The difference in the number of packets transmitted from the air-to-ground and ground-to-air is likely due to the requirement that the DSRC systems need to have a GPS fix in order to transmit a position packet and that vehicle maneuvering can sometimes confound GPS reception. From Figure 19 it can also be seen that between 2 and 100 data packets were transmitted for the air-to-air data analysis for ranges approximately from 0.2 to 1.6 km. The very low number of packets transmitted for ranges less than 200 m was due to the presence of the 152 m (500 ft) wide no-fly zone.

Figure 20 presents the percentage of packets received results. Flight test results for multiple flights were combined to provide the results presented in Figure 20. From Figure 20 it can be seen that the percentage of packets received by the Tempest from the GCS was approximately 80% at 100 m, 50% at 200 m, and reaches 55% at 300 m then decreases to approximately 20% at 900 m. The percentage of packets transmitted from the Tempest to the GCS is approximately 90% then decreases to 50% at approximately 600 m then decreases to 20% around 800 m. There is a slight increase in the percentage of packets received by the GCS from the Tempest at 900 m.

The percentage of packets received by the Tarot is approximately 90% at 100 m and decreases to 50% at 500 m then decreases to 30% at 600 m. The percentage of packets received by the GCS from the Tarot was approximately 90% at 100 m then decreased to approximately 70% at 500 m and then increased to 85% at 600 m.

The percentage of packets received from the GCS to the Mig was approximately 70% at 100 m and decreased to 50% by 200 m. By 600 m the percentage of packets received from the GCS to the Mig was almost zero but did increase to 30% at 800 m. Results for the Mig to the GCS were very similar to those for the GCS to the Mig.

Air to air results indicate that the percentage of packets received by the Tarot from the Tempest was approximately 50% at 200 m, increased to approximately 55% at 300 m, then decreased to 10% by 600 m and eventually became zero but not until approximately 1.1 km.

Results for the percentage of packets received by the Mig from the Tempest was 100% at 200m and then decreased quickly to zero at 400 m. At 500 m the percentage of packets received by the Tempest from the Mig increased to 10% at 500 m, then became zero again by 800 m. Results for the percentage of packets received by the Tempest from the Mig were similar to the Mig to the Tempest.

The percentage of packets received by the Tempest from the Tarot was approximately 75% at 200 m, then decreased to 50% at approximately 400 m. The percentage of packets received by the Tempest from the Tarot then decreased to 20% at 600 m, increased to 30% at 800 m them decreased to zero at 1.1 km. If more than 50% of the packets transmitted need to be received for effective air traffic deconfliction, then the effective range becomes more like 400 m. This amount of range may be inadequate for vehicles approaching each other at speeds greater than 10 m/s assuming a 30 second warning time.

Overall observations from the DSRC flight testing results are that air-to-ground performance is similar to ground-to-air for the same vehicle for a range of distances. The exception to this is for the Tarot with much better air-to-ground performance than ground-to-air as shown in Figure 20. At the maximum range, air to ground and ground to air reception performance was approximately equivalent for the Tempest and Mig. The best air-to-air performance was observed for the Tarot to the Tempest with more than 50% of the

packets received for ranges up to 400 m. This could be due to the combination of antennas involved with this particular transmission path (i.e. dipole to patch). Packet transmission to/from the Mig to the Tempest and/or vice versa was much less than the performance to/from the Tarot to Tempest potentially due to the presence of the carbon strip in the Mig that could have degraded antenna performance for that vehicle.

Comparisons of ground-to-ground performance to ground-to-air, air-to-ground, and air-to-air provide further insight into the DSRC performance. Comparing Figures 18 and 20 reveal that ground-to-ground packet transmission performance was superior compared to air-to-ground, ground-to-air, or air-to-air for ranges less than approximately 600 m in general. However, for ranges greater than 600 m, air-to-ground, ground-to-air, and air-to-air were somewhat better for the Tempest and Tarot with maximum transmission ranges up to 1.1 km vs 0.7 km for ground to ground.

It is hypothesized that the difference in the ground-to-ground vs the air-to-ground, ground-to-air and air-to-air results may be explained by the differences in test methods. For the ground-to-ground testing, the Mobile Unex box was oriented with the normal to the surface of the Taoglass antenna aimed at the test aircraft. For the Tempest ground to ground testing, the same orientation was used producing a highly advantageous antenna alignment as suggested in Figure 8. Stated another way, the “z” vectors of the Taoglass antennas were aimed at each other for the Mobile Unex box and Tempest aircraft. For flight testing, the orientation of the antennas was variable and based on the direction the vehicle was pointing. It also needs to be noted that the method of flight testing can incur some artifacts due to the flight paths selected.

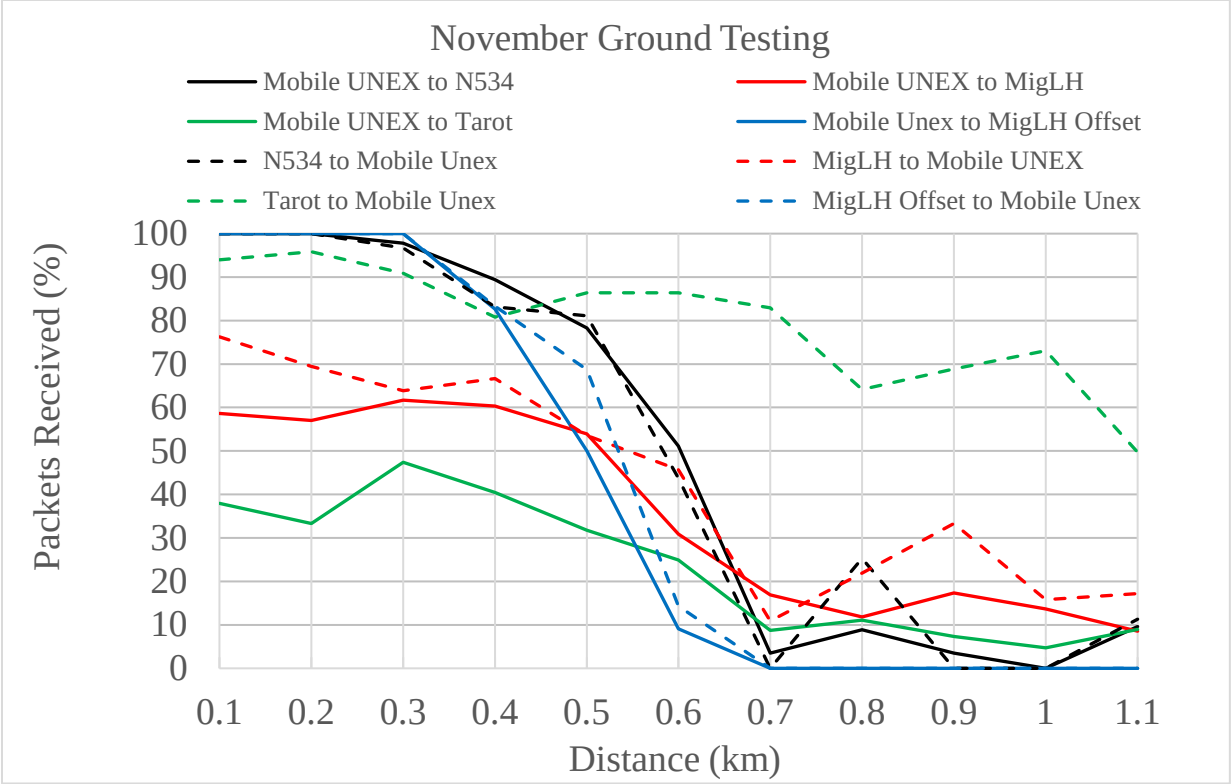

Figure 18 - Results for ground range testing of DSRC V2V equipment.

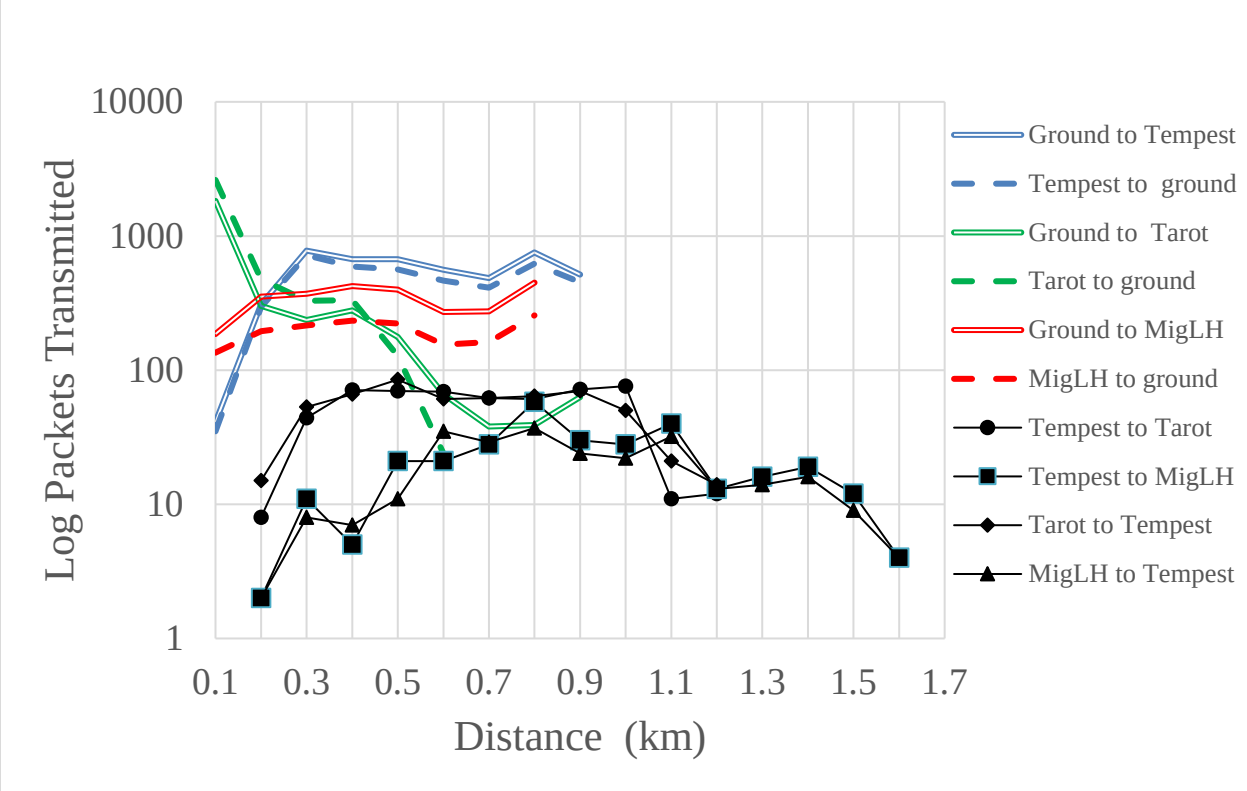

Figure 19 - Distribution of data points for DSRC V2V flight testing.

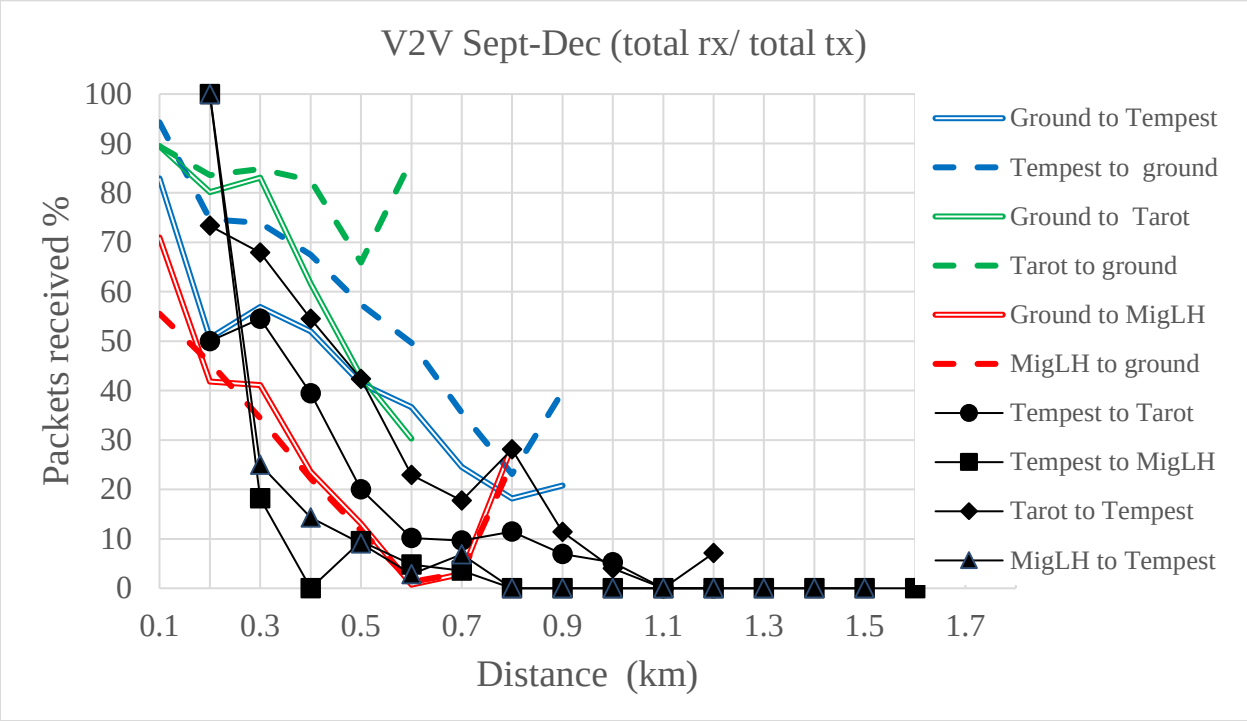

Figure 20 - Results from flight testing of DSRC V2V equipment.

Botlink 4G flight testing

Results for the Botlink 4G flight testing are provided in this section.

Figure 21 presents the total time where the Tempest was not connected to any cell tower along with the time where there was no cell tower identification (CID) in the recorded data. It is considered that both conditions (no connected cell tower and no CID) were indicative of a no-link condition. It can be seen from Figure 21 that the amount of time of no cell link varied from a maximum of 100 seconds for Flight 39 down to zero seconds for Flight 53. It is hypothesized that the method of vehicle preflight was partially responsible for some of the variation in the results. For Flight 53 the Tempest was moved directly from its assembly stand, where it was positioned approximately 3 ft above the ground, to the launcher rail, where it was approximately 1 ft off the ground and then launched. The other flights involved placing the Tempest directly on the ground for more than a minute prior to launch. In addition, the large amount of no link for Flight 39 is likely due to an extended amount of manual maneuvering for that flight with almost no time in auto mode.

Figure 22 presents the total number of cell phone towers connected to the Tempest for each flight. It can be seen from Figure 22 that the Tempest was connected to an average of approximately 2 or 3 towers. The highest number of connected cell towers were for Flight 48 with a mean of more than 3 with only approximately 20% of the time connected to less than 2 towers. Note that flight 48 was flown at the highest cruising altitude of 230 m (755 ft). Lowest number of connected towers was for Flight 49 with an average closer to 2 towers that was flown with the lowest cruising altitude of 170 m (556 ft).

Figure 23 presents the mean distance from the Tempest to the primary connected cell phone tower. From Figure 23 it can be seen that the mean distance was approximately 5.5 miles for most flights indicating that the Tempest was communicating with the closest available tower (refer to Table 1 for the cell tower data base). The standard deviation bars in Figure 23 indicate the variation of cell phone towers connected to for each flight. The largest variation was for Flight 39 which had a large amount of manual maneuvering and almost no auto mode. Flight 49 had the least variation in distance with much of that due to the distance covered by the vehicle in flight. The maximum distance to the connected cell tower recorded for all flights herein was 16.4 miles observed for Flight 39.

Figure 24 presents mean RSRP for all flights. Reference 12 indicates that good to excellent RSRP values are greater than -105 dBm. Poor RSRP is considered to be less than -120 dBm. Figure 24 indicates that RSRP in the good to strong range. Figure 25 presents real-time RSRP as a function of altitude for Flight 53. It can be seen from Flight 53 that RSRP was in the poor range at low altitudes when the vehicle is being prepared for flight. RSRP increases until the Tempest reached approximately 100 ft (30 m) altitude then was fairly constant throughout the flight. The majority of the flight in auto mode occurred at approximately 550 ft (168 m) as indicated by the large cluster of data points at that altitude.

Mean reference signal received quality is presented in Figure 26. Reference 12 indicates that good to excellent RSRQ exist for values greater than -15 dBm. Fair to poor RSRQ values exists for RSRQ ranges less than -15 dBm. Figure 26 reveals that mean RSRQ was predominantly below the fair to poor range for all flights. However, many flights had good to strong values for RSRQ for at least part of time as indicated by the standard deviation bars in Figure 26. Figure 27 presents real-time RSRQ as a function of altitude for Flight 53. Unlike RSRP, RSRQ does not appear to be a function of altitude. The best results for RSRQ appear to be during the mid-altitudes where the vehicle was climbing to or descending from cruise altitude.

Overall, results for the 4G cell link indicate a potentially usable system for command and control. Results for distance to the connected tower appear to indicate that the directionality of the Taoglass antenna may cause some issues that might be resolved with a more omnidirectional antenna. This is supported by the larger variation for Flight 39 which included a large amount of manually-controlled vehicle maneuvering. It was somewhat surprising that the data indicates that the maximum range to a connected tower was greater than 16 miles. However, in general, the Botlink 4G system was connected to the closest tower which was 5.2 miles away with good to strong RSRP. In addition, the system was also connected to more than 2 cell towers most of the time which provides some level of redundancy and enhances the potential use of this method of C2 for sUAS. It is considered that a higher number of connected towers (i.e.; 3 or 4) may be required for adequate C2. Another observation was that in areas with very poor cell coverage, such as those tested in a rural environment, reliable communications with the vehicle in close proximity to the ground may not be possible. It needs to be recognized that much of a sUAS operations occurs on the ground during preflight, launch and recovery operations. The required performance for communication links based on phase of flight need to be established.

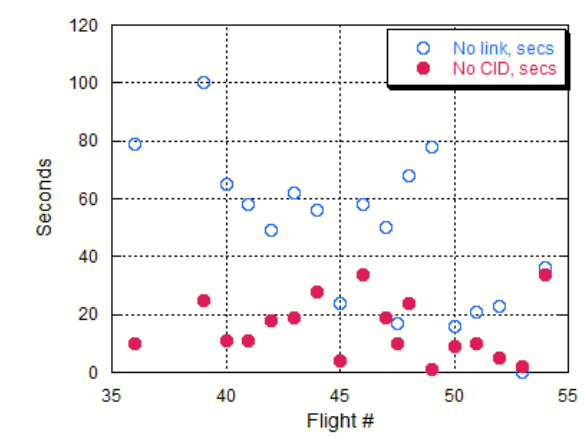

Figure 21- Total time with no link and time with no cell ID for flights.

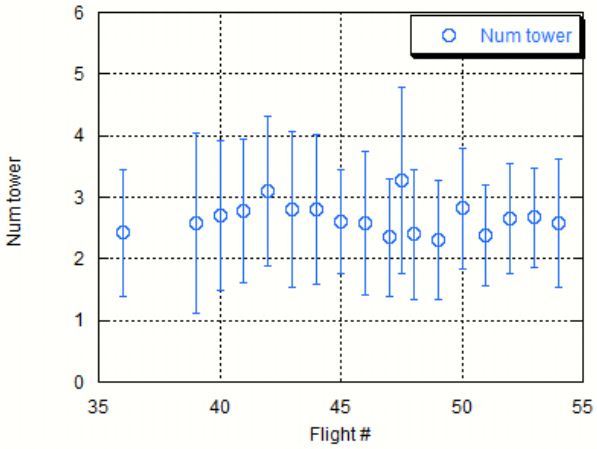

Figure 22 - Number of connected towers for all flights. Error bars are one standard deviation.

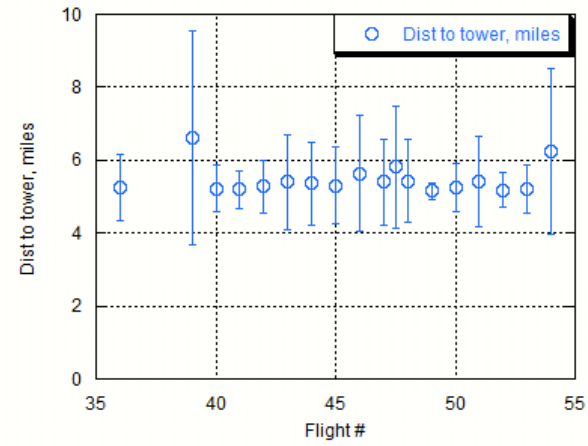

Figure 23- Mean distance to the primary connected tower to the Tempest aircraft for all flights Error bars are one standard deviation.

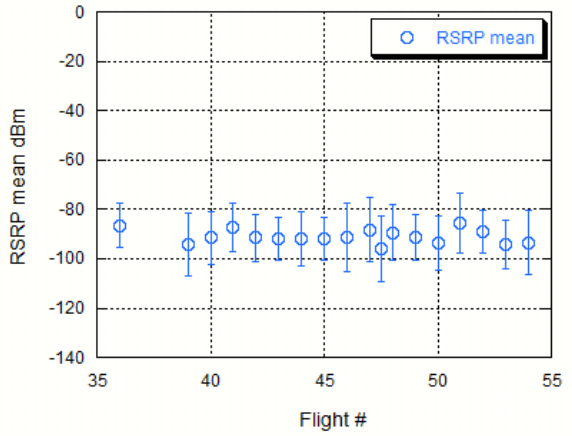

Figure 24 - Mean Reference Signal Received Power for all flights. Error bars are one standard deviation.

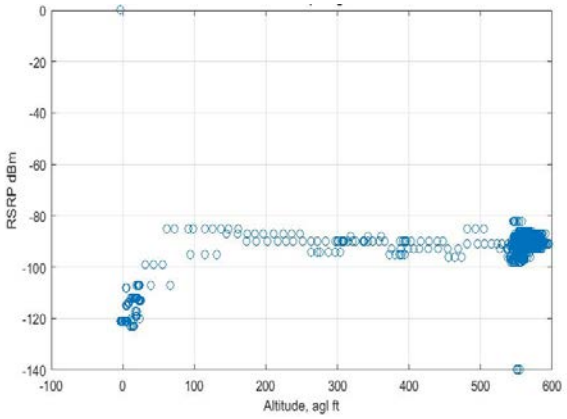

Figure 25- Real time RSRP vs altitude for Flight 53.

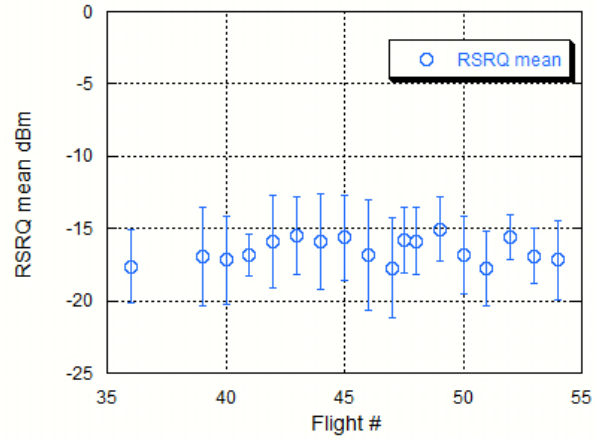

Figure 26 - Mean Received Signal Reference Quality for all flights. Error bars indicate are one standard deviation.

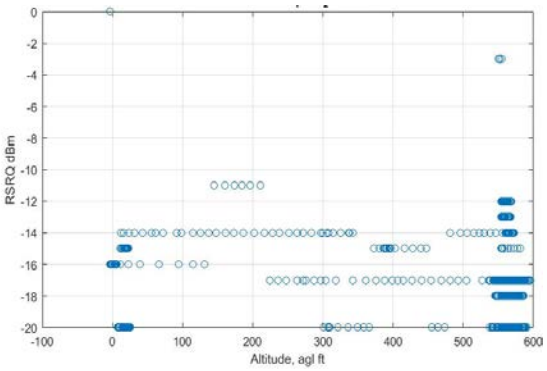

Figure 27- Real-time RSRQ vs altitude for Flight

IOD discussion and initial results

Image-based Object Detection results are provided in this section. High-resolution position-correlated video were acquired for a range of separation distances from 500 ft (152 m) out to approximately 1 mile (1.6 km).

Preliminary results indicate improved detection at greater ranges for above-the-horizon detection as shown in Figures 28 through 30 compared to previous results with lower ppd systems as presented in Reference 8. Figure 28 shows positive detection of the Tempest at approximately 780 m (2,559 ft) heading towards the Tarot Hexacopter. Figure 29 shows the Tempest performing a high-profile maneuver with positive detection. Finally, figure 30 shows the Tempest aircraft with a tangential heading to the Hexacopter with three false positives at a range of 260 m (853 ft).

Future IOD work include:

1. Synchronizing video data and flight logs from flight controllers for the entire dataset so that information regarding the pose, separation distance, cross-sectional area exposed to the camera, and velocity may be used to interpret the IOD results.
2. The implementation of a Kalman filter to further suppress false positives for the optical-flow method.
3. The implementation of IOD algorithms used in Reference 9 used for manned aircraft testing.
4. Design of baseline IOD system for sUAS to include: camera(s), lens, algorithm, and computer system.
5. The implementation of Convolution Neural Network for potential intruder classification.

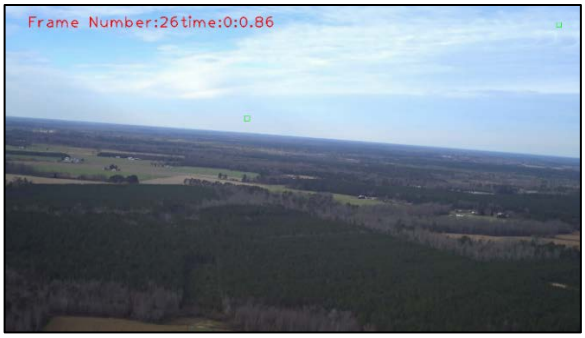

Figure 28: The Tempest (the intruder sUAS) is detected in the middle of the image.

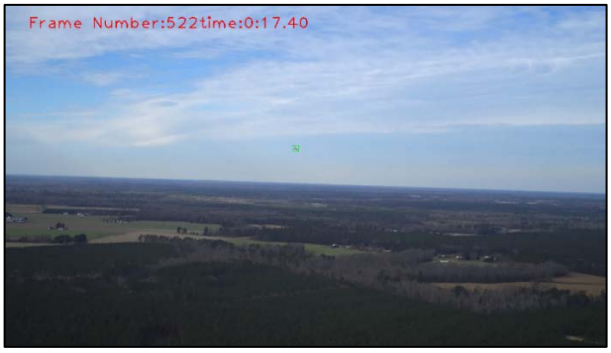

Figure 29: An example of a detection without false positives.

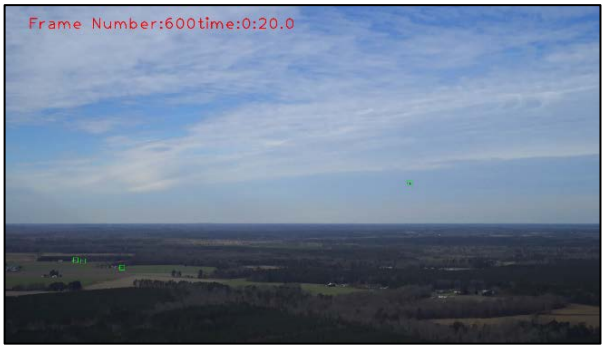

Figure 30: A typical frame with positive detection with 3 false positives.

Safeguard

Two flights were completed using the Tempest-1 with Safeguard installed and operational. Flight paths are shown in Figures 30 and 31, with the geo-fence stay-in test case boundary overlaid, as well as the state (outside or inside) as determined by Safeguard during the flights. For these tests, only a stay-in boundary was used. Further, a relatively small area was defined with a complex irregular shape. This allowed the testing of many boundary crossings at many different approach angles and speeds, as well as climbing and descending.

As shown in the figures, for both flights, Safeguard correctly identified each point as inside or

outside the boundary. For Tempest-1 Flight 27, this corresponded to 2468 total measurements and 1410 in-flight measurements (23.5 minutes). For Tempest-1 Flight 28, this corresponded to 2233 total measurements and 1370 in-flight measurements (22.8 minutes). As indicated in the zoomed-in portions of Figure 30 (a-d), measurements near the boundaries were also correctly identified. For Flight 27 the minimum distance-to-boundary was 0.15 m. The variance in measure-to-measure distances is due to differences in vehicle velocity as expected, given a 1 Hz update rate. The clustering of points, such as shown in Figure 30 (d), is due to the overlay of multiple laps flown by the vehicle once reaching the flight path altitude of 200 m (656 ft). During these flights, speed ranged from 0 to 32.6 m/sec (0 to 73 mph).

A higher-level function within Safeguard predicts boundary violations such that the pilot (or auto-pilot) can be warned in time to make a contingency maneuver that avoids breaching a fence. Safeguard has the ability to signal when flight termination may be necessary to keep the vehicle from leaving a fenced area for a case where violation is eminent and the pilot or auto-pilot has not intervened appropriately. Both the warning and termination signals are issued based on Safeguard configuration settings established prior to flight by the operator. These include buffer sizes, scale factors, and/or aircraft aerodynamic model coefficients.

For the two test flights with the Tempest, these were all set very conservatively and the test boundary was defined as a relatively small region given the flight performance capability of the Tempest. This resulted in only small segments of time where predictive warnings were generated. One example is shown in Figure 32 for Flight 27. Here, as the vehicle approaches a boundary, the warning signal becomes active first (blue '+' symbol), then the terminate signal becomes active (red '*' symbol). For this version, terminate is defined as points wherein the vehicle is predicted to cross a boundary even if all power is cut from the motors (i.e. the ballistic trajectory will take the vehicle beyond the boundary). In the example shown, the vehicle is slowing and descending (to land), so warnings and terminate signal transitions can be seen. These transitions would not be seen during the higher altitude high-speed flying as the stay-in region defined was too small to test these transitions.

All of this data helps to validate the formally-verified function within Safeguard that determines inside/outside for any point with a high-degree of assurance (i.e. very low probability of missed-detection and false alarm) as described in Reference 13.

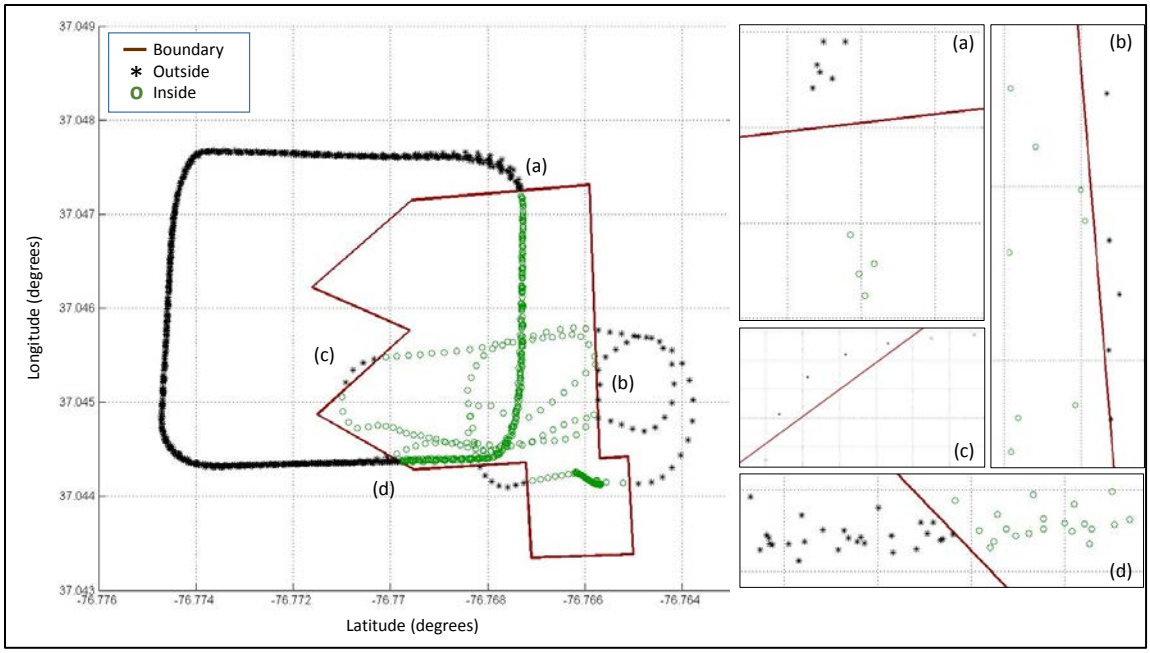

Figure 30. Safeguard test results (Flight 27)

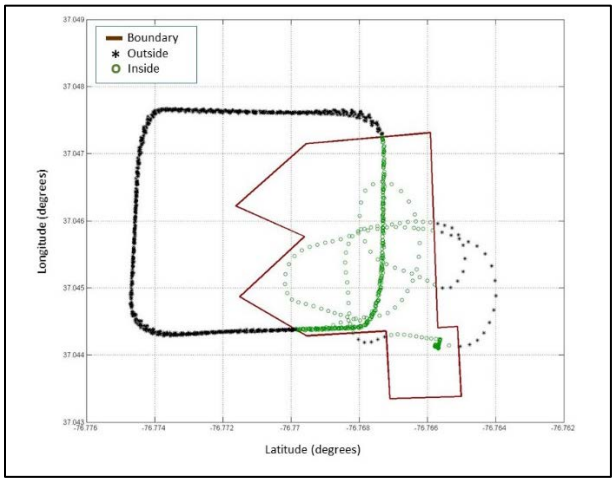

Figure 31. Safeguard test results (Flight 28)

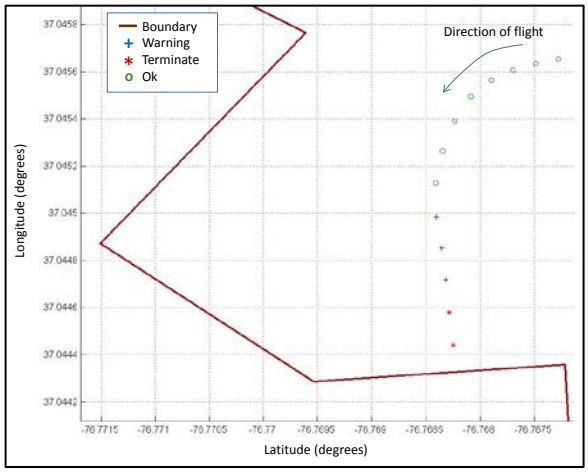

Figure 32. Sample predictive warning case (Fight 27).

Conclusions

A series of ground and flight tests were completed to address the potential use of Dedicated Short Range Communications (DSRC) systems for potential sense and avoid small unmanned aerial systems (sUAS) applications, evaluation of the use of cellular 4G systems to provide vehicle control, to obtain high-resolution video imagery in support of image-based optical detection sense and avoid systems, and acquisition of data in support of development of an autonomous range containment system.

The following conclusions can be made regarding the results presented. One conclusion is that the effective range of the DSRC system to transmit and receive packets to other aircraft is limited to ranges less than 1 km. However at this range only approximately 10% of the packets were successfully received by the other aircraft. If more than 50% of the packets transmitted need to be received for effective air traffic deconfliction, then the effective range becomes more like 400 m. This amount of range may be inadequate for vehicles approaching each other at speeds greater than 10 m/s assuming a 30 second warning time.

Results for 4G link testing in a rural environment indicate that some periods of signal loss were experienced as tested. However, those periods of signal loss occurred more frequently on the ground likely a result of very low reference signal received power (RSRP) while the vehicle was directly on the ground. RSRP increased quickly as altitude increased becoming good to excellent for a large majority of the time. However, signal quality as indicated reference signal received quality (RSRQ) remained fair to poor for much of the time. Vehicle maneuvering can affect cell reception due to observed antenna non-uniformity. While the closest cell tower was predominantly used as the primary connected tower, data indicates that many towers were connected to the vehicle throughout the flight test. The maximum distance observed for a connected tower was more than 16 miles away. It is considered that a combination of short-range direct communications link, such as a 900 MHz link, combined with a 4G based link could potentially provide required sUAS command and control (C2) functionality in rural areas.

Initial results for post-processed Image-based Object Detection (IOD) indicate that sUAS can be detected at ranges up to 780 m (2,559 ft). This result is significantly improved from previous work that used a larger field of view (FOV) lens with much lower resolution.

Finally, testing of the highly-assured vehicle containment system known as Safeguard system was performed at speeds commensurate to fixed-wing sUAS aircraft. Results from this testing indicated appropriate performance of the system to correctly identify the zones of operation (stay in this application) and provide warning and vehicle terminate messages.

Future work

Future work for DSRC testing should evaluate both higher transmit power levels along with more optimized antennas to improve the range of communications. Future work is also recommended to further explore the capabilities of 4G cell link technologies to provide required communications performance. Results for suburban and urban areas, with assumed higher-density of cell towers and potential obstructions would complement the current data. Further work is being performed to fully analyze results for IOD algorithms as well as to define a baseline IOD system (i.e. camera, lens, algorithm, and computer) applicable for sUAS. Subsequent testing of a baseline IOD system should be performed. Failure mode effects analysis should be performed to compare and contrast an external geofence containment system (Safeguard) to one that hosts the system internally on the autopilot. Lastly, subsequent testing of Safeguard should be performed at potentially higher speeds and more complex boundaries. Fixed-wing vehicle dynamics during Safeguard terminations should also be evaluated to quantify the potential dispersions.

References

1. Kopardekar, P.; Rios, J.; Prevot, T.; Johnson, M.; Jung, J.; Robinson, J.: *Unmanned Aircraft System Traffic Management (UTM) Concept of Operations*. AIAA Aviation Conference, 2016.
2. Wilson, M.; *Ground-Based Sense and Avoid Support for Unmanned Aircraft Systems.* 28th International Congress of the Aeronautical Sciences, ICAS 2012.
3. Federal Aviation Administration, Automatic Dependent Surveillance-Broadcast (ADS-B)/ADS-B Rebroadcast (ADS-R) Critical Services Specification, FAA-E-3011, Revision A. January 7, 2015.
4. Guterres, R.; Jones, S.; Orrell, G.; Stain, R.: *ADS-B Surveillance System Performance with Small UAS at Low Altitudes.* AIAA SciTech Forum, January, 2017, Grapevine Texas.
5. Harding, J., Powell, G., R., Yoon, R., Fikentscher, J., Doyle, C., Sade, D., Lukuc, M., Simons, J., & Wang, J. (2014, August). *Vehicle-to-vehicle communications: Readiness of V2V technology for application.* (Report No. DOT HS 812 014). Washington, DC: National Highway Traffic Safety Administration.
6. Geiver, L: Using Innovative Satellite, 5G system, sUAS goes BVLOS in VA. UAS Magazine, April 13, 2017.
7. Qualcomm Technologies: *LTE Unmanned Aircraft Systems.* Trial report. May 12, 2017.
8. Dolph, C.; Logan, M.; Glaab, L.; Vranas, T.; McSwain, R.; Johns, Z.; Severance, K.: *Sense and Avoid for Small Unmanned Aircraft Systems*, in *AIAA Information Systems-AIAA Infotech@ Aerospace*, Grapevine, 2017.
9. Minwalla, D. Tuplan, N. Belacel, F. Famili and K. Ellis, Detection of Airborne Collision-Course Targets for Sense and Avoid on Unmanned Aircraft Systems Using Machine Vision Techniques, Unmanned Systems, vol. 4, no. 4, pp. 1-18, 2016.
10. Gilabert, R.; Dill, E.; Hayhurst, K.; and Young, S.: *Safeguard – Progress and Test Results for A Reliable Independent On-board Safety Net for UAS*, in Proceedings of 36th AIAA/IEEE Digital Avionics Systems Conference, St. Petersburg, FL, September 2017.
11. Dill, E., Young, S., and Hayhurst, K., *Safeguard – An Assured Safety Net Technology for UAS*, Proceedings of 36th AIAA/IEEE Digital Avionics Systems Conference, September 2016.
12. Industrial Networking Solutions Tips and Tricks: Making Sense of Signal Strength/Signal Quality Readings for Cellular Modems.
13. Narkawicz, A. J.; and Hagen, G. E.: *Algorithms for Collision Detection Between a Point and a Moving Polygon, With Applications to Aircraft Weather Avoidance*. AIAA Aviation 2016, June 13-17, 2016, Washington, District of Columbia

Appendix A: Flight run log

All flights performed in support of the V2V-1 flight test effort are contained herein. Column 1(#) is the reference line entry for this log. Column 2 (Date) is the date the flight(s) were completed. Colum 3 (Ops #) is the Ops day counter. Colum 4 (V1) is the 1st vehicle in the run log data entry. Note that flight pairs are entered twice once for each vehicle in the pair. Column 5 is the flight number for that aircraft as logged in its log book. Column 6 (V1 Alt) is the designated auto flight cruise altitude for Vehicle 1 in meters. Column 7 (Flight Time) is Vehicle 1's approximate flight time in minutes. Column 8 (Config) is the configuration for Vehicle 1. Column 9 is the vehicle that was flown with Vehicle 1. Column 10 (V2 Alt) is Vehicle 2's designated cruise altitude in meters. Column 11 (Botlink Data) indicates if valid Botlink data were acquired for Vehicle 1. Column 12 (V2V data) indicates if DSRC Vehicle to Vehicle data were acquired and if so what transmission path was tested (ATG=Air to Ground, ATA=Air to Air, GTA=Ground to Air). Column 13 (Video data) indicates if Image-based Object Detection data were acquired for this flight pair. Column 14 (SG) indicates if Safeguard data were acquired for Vehicle 1.

#	Date	Ops #	V1	V1 flt #	V1 Alt (m)	Flight Time (min)	Config	V2	V2 Alt (m)	Botlink Data	V2V data	Video data	SG
1	8/3/2017	1	Mig-CC	22	200	9	V2V/Camera						
2	8/3/2017	1	Mig-CC	23	200	10	V2V/Camera						
3	8/25/2017	2	Mig-CC	24			V2V/Camera						
4	8/25/2017	2	Tempest-1	22		22							Y
5	8/25/2017	2	Tempest-2	35	170	40				Y			
6	9/8/2017	3	Mig-LH	74	200	9	V2V/Camera						
7	9/29/2017	4	Tempest-1	27	240 200 140	20	Safeguard						
8	9/29/2017	4	Tempest-2	36	160 200 250	35	ADS-B/Unex/Botlink on			Y	ATG		
9	10/3/2017	5	Tempest-2	37	200 250	14				Y	ATG		
10	10/3/2017	5	Tempest-2	38	250	16		?		Y	ATG		
11	10/17/2017	6	Mig-CC	25			Baseline						
12	10/17/2017	6	Mig-CC	26			Baseline						
11	10/17/2017	6	Mig-CC	27			Baseline						
12	10/18/2017	7	Tarot-2	4		2	V2V/Camera/Video TX						
13	10/18/2017	7	Tarot-2	5		5	V2V/Camera/Video TX						

#	Date	Ops #	V1	V1 flt #	V1 Alt (m)	Flight Time (min)	Config	V2	V2 Alt (m)	Botlink Data	V2V data	Video data	SG
14	10/18/2017	7	Tarot-2	6		2	V2V/Camera/Video TX						
15	10/18/2017	7	Tarot-2	7		2	V2V/Camera/Video TX						
16	10/18/2017	7	Tarot-2	8	200	13	V2V/Camera/Video TX	Tempest-2				Y	
17	10/18/2017	7	Tarot-2	9	200	3	V2V/Camera/Video TX						
18	10/18/2017	7	Tarot-2	10	200	10	V2V/Camera/Video TX	Tempest-2				Y	
19	10/18/2017	7	Tempest-2	39	230	10	ADS-B/Unex/Botlink on	?		Y	ATG		
20	10/18/2017	7	Tempest-2	40	230	13	ADS-B/Unex/Botlink on	Tarot-2		Y	ATG	Y	
21	10/18/2017	7	Tempest-2	41	170	20	ADS-B/Unex/Botlink on	Tarot-2		Y	ATG	Y	
22	10/19/2017	8	Mig-LH	75	200	10	V2V/Camera	Tempest-2			ATG		
23	10/19/2017	8	Mig-LH	76	200	10	V2V/Camera	Tempest-2			ATG		
24	10/19/2017	8	Mig-LH	77	200	10	V2V/Camera	Tempest-2			ATG		
25	10/19/2017	8	Tempest-2	42	200	24		Mig-LH		Y	ATG		
26	10/19/2017	8	Tempest-2	43	170	16		Mig-LH		Y	ATG		
27	10/19/2017	8	Tempest-2	44	230	18		Mig-LH		Y	ATG		
28	10/31/2017	9	Mig-LH	78	200	11	V2V/Camera	Tempest-2			ATG		
29	10/31/2017	9	Mig-LH	79	200	11	V2V/Camera	Tempest-2			ATG		
30	10/31/2017	9	Mig-LH	80	200	11	V2V/Camera	Tempest-2			ATG		
31	10/31/2017	9	Tempest-2	45	170	20		Mig-LH		Y	ATG		
32	10/31/2017	9	Tempest-2	46	200	20		Mig-LH		Y	ATG		

#	Date	Ops #	V1	V1 flt #	V1 Alt (m)	Flight Time (min)	Config	V2	V2 Alt (m)	Botlink Data	V2V data	Video data	SG
33	10/31/2017	9	Tempest-2	47	230	20		Mig-LH		Y	ATG		
34	11/28/2017	10	Mig-LH	81	200	10	V2V/Camera	Tempest-2			ATG	Shake/Swim	
35	11/28/2017	10	Mig-LH	82	200	11	V2V/Camera	Tempest-2			ATG	Y	
36	11/28/2017	10	Mig-LH	83	200	11	V2V/Camera	Tempest-2			ATG	Y	
37	11/28/2017	10	Mig-LH	84	200	12	V2V/Camera	Tempest-2			ATG	Y	
38	11/28/2017	10	Tempest-1	28	200	11	Safeguard						
39	11/28/2017	10	Tempest-2	48	230	17	ADS-B on	Mig-LH		Y	ATG	Y	
40	11/28/2017	10	Tempest-2	49	170	16	ADS-B off	Mig-LH?		Y	ATG	Y	
41	11/28/2017	10	Tempest-2	50	200	16	ADS-B off	Mig-LH?		Y	ATG	Y	
42	11/28/2017	10	Tempest-2	51	230	17	ADS-B off	Mig-LH?		Y	ATG	Y	
43	11/30/2017	11	Mig-LH	85	200	11	V2V/Camera	Tempest-1			ATG	Y	
44	11/30/2017	11	Mig-LH	86	200	10	V2V/Camera	Tempest-2			ATG	Y	
45	11/30/2017	11	Tempest-1	29	230	22	Safeguard	Mig-LH				Y	Y
46	11/30/2017	11	Tempest-1	30	170	23	Safeguard						Y
47	11/30/2017	11	Tempest-2	52	170	19	ADS-B off	Mig-LH		Y	ATG, ATA	Y	
48	12/7/2017	12	Tarot-2	11	200	14	V2V/Camera	Tempest-2	170		ATG, ATA	Y	
49	12/7/2017	12	Tarot-2	12	200	12	V2V/Camera	Tempest-2	200		ATG, ATA	Y	
50	12/7/2017	12	Tarot-2	13	200	13	V2V/Camera	Tarot-1			ATG, ATA	Dual	
51	12/7/2017	12	Tarot-2	14	200	13	V2V/Camera	Tarot-1			ATG, ATA	Dual	
52	12/7/2017	12	Tempest-2	53	170	20	ADS-B off	Tarot-2		Y	ATG, ATA	Y	

#	Date	Ops #	V1	V1 flt #	V1 Alt (m)	Flight Time (min)	Config	V2	V2 Alt (m)	Botlink Data	V2V data	Video data	SG
53	12/7/2017	12	Tempest-2	54	200	20	ADS-B off	Tarot-2		Y	ATG, ATA	Y	
54	12/7/2017	12	Tarot-1	55				Tarot-2			ATG, ATA		
55	12/7/2017	12	Tarot-1	56				Tarot-2			ATG, ATA		
			55	Vehicle Flt #		734		36					

REPORT DOCUMENTATION PAGE

Form Approved
OMB No. 0704-0188

1. REPORT DATE *(DD-MM-YYYY)*	2. REPORT TYPE	3. DATES COVERED *(From - To)*
1-04-2018	Technical Memorandum	

4. TITLE AND SUBTITLE

Small Unmanned Aerial System (UAS) Flight Testing of Enabling Vehicle Technologies for the UAS Traffic Management Project

5a. CONTRACT NUMBER

5b. GRANT NUMBER

5c. PROGRAM ELEMENT NUMBER

6. AUTHOR(S)

Glaab, Louis J.; Dolph, Chester V.; Young, Steve, D.; Coffey, Neil C.; McSwain, Robert G.; Logan, Michael J.; Harper, Donald E.

5d. PROJECT NUMBER

5e. TASK NUMBER

5f. WORK UNIT NUMBER

334005.05.10.07.01

7. PERFORMING ORGANIZATION NAME(S) AND ADDRESS(ES)

NASA Langley Research Center
Hampton, VA 23681-2199

8. PERFORMING ORGANIZATION REPORT NUMBER

L-20914

9. SPONSORING/MONITORING AGENCY NAME(S) AND ADDRESS(ES)

National Aeronautics and Space Administration
Washington, DC 20546-0001

10. SPONSOR/MONITOR'S ACRONYM(S)

NASA

11. SPONSOR/MONITOR'S REPORT NUMBER(S)

NASA-TM-2018-219816

12. DISTRIBUTION/AVAILABILITY STATEMENT

Unclassified--
Subject Category 03
Availability: NASA STI Program (757) 864-9658

13. SUPPLEMENTARY NOTES

14. ABSTRACT

Small unmanned aerial systems (sUAS) have been studied and results indicate that there is a large array of highly-beneficial applications. These applications are too numerous to list, but include search and rescue, fire spotting, precision agriculture, etc. to name a few. Typically sUAS vehicles weigh less than 55 lbs and will be performing flight operations in the presence of manned aircraft and other sUAS. Certain sUAS applications, such as package delivery, will include operations in the close proximity of the general public. The full benefit from sUAS is contingent upon the resolution of several technological areas to enable free and wide-spread use of these vehicles. Technological areas in question include, but are not limited to: autonomous sense and avoid and deconfliction of sUAS from other sUAS and manned aircraft, communications and interfaces between the vehicle and human operators, and high-reliability autonomous systems. The NASA UAS Traffic Management (UTM) project is endeavoring to develop a traffic management system and concept of operations for these types of vehicles. An extensive sUAS flight test effort was performed to partially address vehicle-related technological areas and to shape an understanding of future developmental and test efforts for vehicles intended to use the UTM traffic management system.

15. SUBJECT TERMS

4G; C2; DSRC; Flight Testing; Image-based Object Detection; Safeguard; sUAS

16. SECURITY CLASSIFICATION OF:			17. LIMITATION OF ABSTRACT	18. NUMBER OF PAGES	19a. NAME OF RESPONSIBLE PERSON
a. REPORT	b. ABSTRACT	c. THIS PAGE			STI Help Desk (email: help@sti.nasa.gov)
U	U	U	UU	33	19b. TELEPHONE NUMBER *(Include area code)* (757) 864-9658